Orbital-selective insulator-metal transition in V_2O_3 under external pressure

M. S. Laad
Department of Physics, Loughborough University, Loughborough LE11 3TU, United Kingdom

L. Craco and E. Müller-Hartmann
Institut für Theoretische Physik, Universität zu Köln, 77 Zülpicher Straße, 50937 Köln, Germany
(Received 12 May 2005; revised manuscript received 9 November 2005; published 12 January 2006)

We present a detailed account of the physics of vanadium sesquioxide (V_2O_3), a benchmark system for studying correlation-induced metal-insulator transition(s). Based on a detailed perusal of a wide range of experimental data, we stress the importance of multiorbital Coulomb interactions in concert with first-principles local-density approximation (LDA) band structure for a consistent understanding of the insulator-metal (IM) transition under pressure. Using LDA+DMFT (dynamical mean-field theory), we show how the IM transition is of the orbital selective type, driven by large changes in dynamical spectral weight in response to small changes in trigonal field splitting under pressure. Very good quantitative agreement with (i) the switch of orbital occupation and (ii) $S=1$ at each V^{3+} site across the IM transition, and (iii) carrier effective mass in the paramagnetic phase, is obtained. Finally, using the LDA+DMFT solution, we have estimated screening-induced renormalization of the local, multiorbital Coulomb interactions. Computation of the one-particle spectral function using these screened values is shown to be in excellent quantitative agreement with very recent experimental (photoemission and x-ray-absorption spectroscopy) results. These findings provide strong support for an orbital-selective Mott transition in paramagnetic V_2O_3.

DOI: 10.1103/PhysRevB.73.045109 PACS number(s): 71.28.+d, 71.30.+h, 72.10.−d

I. INTRODUCTION

Correlation-driven metal-insulator transitions have remained unsolved problems of solid-state theory of electrons in solids for more than five decades. The pioneering work of Mott,[1] and of Gutzwiller,[2] Kanamori,[3] and Hubbard[4] involved a detailed exposition of the view, suggesting that description of such phenomena lay outside the framework of band theory. Subsequent, more recent developments, including discovery of high-T_c superconductors, rare-earth-based systems, colossal magnetoresistive oxides along with whole families of other systems have shown that strong electronic correlations give rise to widely unanticipated, fundamentally different types of metallic behaviors, namely, non-Fermi liquid metals. A host of very careful studies now clearly show that these anomalous responses seem to be correlated with the existence of a correlated metallic state on the border of a Mott insulator in d-band oxides,[5] or to a metallic state in proximity to a localization-delocalization transition of f-electrons in rare-earth compounds.[6]

The corundum lattice-based (see Fig. 1) transition-metal (TM) oxide system vanadium sesquioxide (V_2O_3) has been of interest for more than five decades as a classic (and by now a textbook) case of an electronic system with $S=1/2$ local moments at each site exhibiting the phenomenon of the correlation-driven Mott-Hubbard metal-insulator transition (MIT).[1,4] Widely accepted wisdom has it that this is one of the few cases where modeling, in terms of a simple one-band Hubbard model, is appropriate. Over the last few years, experimental and theoretical work has forced a revision of this view, leading on the one hand to a spurt of different approaches, and on the other to an expansion of our perception of what is new and important in the physics of transition-metal oxides, in general. Specifically, taken by themselves as well as in combination with properties of other systems, such as ruthenates, colossal magnetoresistance manganites, etc., these recent studies force one to refocus the attention in terms of the strong coupling and interplay of spin and orbital degrees of freedom (not to be confused with the usual spin-orbit coupling, though that may also be relevant in some situations) and of their combined influence on the nature of charge and spin dynamics in TM oxides.

In what follows, we aim to present a far-from-complete view of the questions that are posed by these recent studies. Focusing our attention to the $3d^2$ vanadium oxide, V_2O_3, we will start with a somewhat detailed perusal of earlier work, review key recent experiments, and follow them up with a discussion of their implications for theory. Finally, we will suggest a rather detailed scenario for correlation-induced metal-insulator transitions in V_2O_3 that ties together essential experimental constraints in one picture. In doing so, we will give a detailed description of our theoretical modeling, using a combination of the local-density approximation (LDA) combined with multi-orbital dynamical mean-field theory (DMFT) using the iterated perturbation theory (IPT) as the "impurity" solver.

In the first part, we will confine ourselves to summarizing known and not so well-known experimental results on the effect of external pressure and Cr doping (see Fig. 2) on the thermodynamic and transport properties of V_2O_3 along with the magnetic and orbital structure (and their changes) across the metal-insulator transition.

In the second part, we will first review the earlier theories for the MIT in terms of the one-band Hubbard model as well as the more recent multiband Hubbard model (which allows a description in terms of a $S=1$ model). Finally, we will propose a scenario: one where the abrupt change in the char-

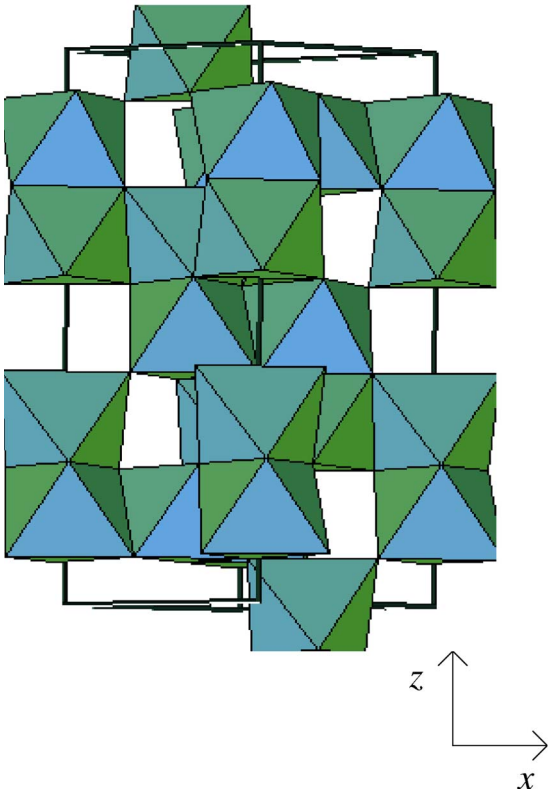

FIG. 1. (Color online) Three-dimensional view of the corundum lattice structure of V_2O_3. The crystallographic (z,x) axes are depicted on the lower right side in the figure.

acter of spin (and presumably also orbital) correlations across the MIT is described within the strong correlation scenario. In particular, we will show how a two-fluid (i.e., orbitally selective) description can be derived from first principles and demonstrate how the properties of V_2O_3 can be understood in this scenario.

II. EXPERIMENTAL REVIEW

The magnetic structure of V_2O_3 has been measured a long time ago.[8] Its interpretation has however remained a subject of controversy. The robust aspects are the antiferroinsulator (AFI) is characterized by antiferromagnetic (AF) order, which spontaneously breaks the crystal symmetry of the corundum lattice- and in modern parlance, it corresponds to the C-type AF order[9] with one ferromagnetic (F) and two AF bonds in the hexagonal plane. The vertical vanadium-vanadium (V-V) pairs (with V^{3+}) form dimers in the solid (see Fig. 3); these are aligned antiferromagnetically with the inplane V-V pairs, and ferromagnetically with other vertical V-V pairs. In terms of these dimers, the corundum lattice can be viewed as a distorted simple cubic lattice (see Fig. 1). Based on the $S=1/2$ picture of Castellani *et al.*, the spin waves were "characterized" in terms of a Heisenberg-like model.[9] This was a commonly accepted picture for almost two decades, until recent experimental results forced one to reanalyze it. These are as follows:

(i) Change of magnetic correlations across the AFI to AF-metal (AFM) phase transition in $V_{2-y}O_3$. The AFM is characterized by incommensurate order with $\mathbf{Q}\|c$, in contrast to that for the AFI, characterized by $\mathbf{Q}=(1/2,1/2,0)$ (hexagonal notation). Furthermore, abrupt jump of the crystal volume (without change of symmetry) is also observed across the paramagnetic-insulator paramagnetic-metal (PI-PM) transition at higher T.[10] The c-axis distance decreases abruptly at the PI-PM transition, while the a-axis distance slightly increases, and this change needs to be correlated with the conductivity jump at the transition (see below).

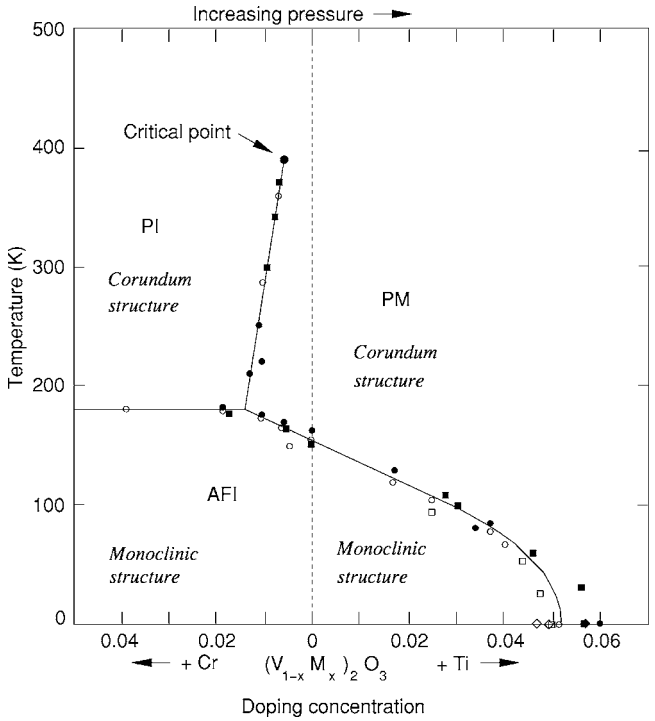

FIG. 2. Phase diagram of $V_{2-x}M_xO_3$ with M=Cr,Ti, showing the AFI, PI, and PM phases as a function of chemical pressure (x) in the temperature "pressure" plane; data points are taken from Ref. 7.

(ii) Recent x-ray experiments by Park *et al.*[11] have revealed the existence of an admixture of $(e_{g1}^{\pi},e_{g2}^{\pi})$ and (e_{gi}^{π},a_{1g}) with $i=1,2$ and a spin $S=1$ on each V site, in contrast to the $S=1/2$ proposed in Ref. 9. In addition, large differences in their ratio have been found in the AFI, PI, and PM phases. In particular, this ratio is $(e_{g1}^{\pi},e_{g2}^{\pi}):(e_{gi}^{\pi},a_{1g})$ is 2:1 in the AFI, 1.5:1 in the PI, and 1:1 in the PM phase. This provides a direct proof of the crucial role of strong multiorbital (MO) correlations for understanding the MIT in V_2O_3. Furthermore, the role of the trigonal field is also clearly important; it acts like an effective "magnetic field" in the orbital sector, and its changes across the MIT determine the changes in occupations of the t_{2g} orbitals in each phase, much in the same way as the magnetization of a paramagnet is a function of the external field in a spin system.

(iii) Optical spectroscopy provides a detailed picture of charge dynamics. Careful studies by Thomas *et al.*[12] reveal all the characteristics of a strongly correlated system: an "upper Hubbard band" (UHB) feature with a threshold in the AFI (and PI), and a sharp, quasi-coherent feature, along with an intense mid-infra-red peak and the remnant of the UHB on the PM side. Calculations within the framework of a

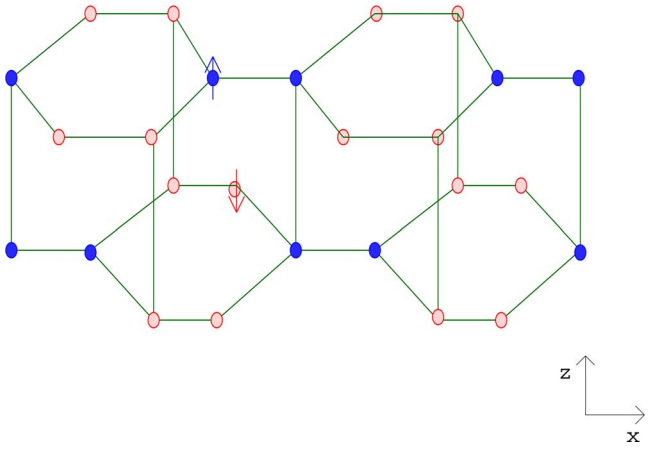

FIG. 3. (Color online) Crystal structure of V_2O_3 in the low-temperature, antiferromagnetically ordered, monoclinic phase. The arrows indicate the orientations of the spins on each Vanadium site. The crystallographic (z,x) axes are depicted on the lower right side in the figure.

$S=1/2$, one-band Hubbard model[13] claim to obtain very good agreement with the observed spectra. However, to achieve this, the Hubbard U has to be changed by a factor of 2 on going from the PI to the PM state, which is hardly conceivable. Alternatively, the effective hopping, or the degree of itinerance, should increase in the metallic state, leading to a change in the effective U/t value, and, as is ubiquitous in strongly correlated scenarios, to a large transfer of spectral weight. In particular, given (i) and (ii), this should involve carriers coupled to spin-orbital degrees of freedom along with the concomitant lattice distortion.

(iv) Photoemission spectroscopy (PES)[14] reveals further proof of the correlation-driven character of the insulator-metal (IM) transition.

At high T, the data is claimed to be consistent with a "thermally smeared quasicoherent" peak, something within reach of single-site theories. However, it is more conceivable that strong inelastic scattering from coupled spin-orbital excitations gives rise to nonquasiparticle dynamics in the PM phase. At lower T, appreciable changes are observed in the PES spectra across the PI/PM transition, with the characteristic transfer of spectral weight from high to low energy over a scale of almost 4 eV (note that $T_{MI} \simeq 300$ K), implying a drastic rearrangement of electronic states over a wide energy scale.[15] In the PM state, the PES spectrum shows the asymmetric two-peak structure with a Fermi edge (but we draw attention to the fact that this low-energy "peak" is anomalously broad, suggesting nonquasiparticle dynamics), while a clear opening of a spectral gap occurs in the PI phase.

Earlier PES studies across the PI-PM transition have been controversial; in particular, the question of the T-dependence of the low-energy spectral weight was not settled until recently. Quite recently, this question has been answered by the Michigan group,[16] and the T-dependent renormalized and heavily-damped "quasiparticle" contribution has indeed been observed.

Details of the PES spectra at high T are seemingly well captured by a DMFT applied to a multiband Hubbard model in combination with the actual LDA band structure (see below for more details).[15] There are still some discrepancies between LDA+DMFT and experiment at lower $T<400$ K; however, the "quasiparticle peak" is too broad by a factor of 2–3, and the details of the PES line shape in the PI still remain to be calculated. It is possible that screening-induced renormalization of U, etc. needs to be included; however, it is a very difficult task to do this from an *ab initio* starting point. Alternatively, or in concert with the above, the dynamical effect of intersite correlations might be expected to become increasingly important at lower T. Such effects are out of scope of LDA+DMFT, and require extensions to treat dynamical effects of spatial correlations, a more demanding task.

(v) One of the most spectacular hallmarks of the IM transition in V_2O_3 is the sharp jump in conductivity by seven orders of magnitude. Is the jump of $\sigma(T)$[17] driven by a jump in the carrier density at the transition or by an increase in the mobility?[18] Hall-effect measurements would be a probe to answer this question. On the barely metallic (close to the AFI) side ($V_{2-y}O_3$), the Hall constant $R_H(T)$ shows behavior reminiscent of the cuprates;[19] it is strongly T dependent, increasing with decreasing T with a peak around the AF ordering temperature, followed by a drop at lower T. The T dependence gets weaker with increasing metallicity (y). More similarities with the normal state of the high-T_c cuprates are seen in the different T dependences of $\rho(T) \simeq T^{3/2}$ and $\cot \theta_H(T) \simeq aT^2+b$ for small y, which evolves into more conventional FL behavior with increasing y.[19] This is a classic signature of nonquasiparticle dynamics; the differing T dependencies for longitudinal and transverse relaxation rates has no analog in any Fermi-liquid (FL) picture. Such a behavior would mandate strong local-moment scattering in the metallic phase. Given the strong correlation signatures observed globally, a description in terms of vagaries of the Fermi surface is untenable.

A. Summary of experimental results in the PM phase

In conclusion, experimental results reveal very interesting points concerning the nature of the paramagnetic phase of V_2O_3: (i) The PM phase shows strong first-order IM transition. A jump in the $(e_{g1}^{\pi}, e_{g2}^{\pi}):(e_{gi}^{\pi}, a_{1g})$ from 2:1 to roughly 1:1 implying a drastic rearrangement of orbital occupation (leading to paraorbital state?) across the IM transition. The basic dependence of the magnetic superexchange interactions (J_{ij}^{ab}) on orbital occupation and symmetry modifies these as a consequence. PES and dc transport measurements indicate that the PM phase is not describable in a FL framework, but requires a non-FL pseudoparticle interpretation.

(ii) Strong correlation-driven physics as very clearly seen in optics and PES. Since U, U' (respectively, the intra- and interorbital Coulomb interaction terms) and the Hund's rule coupling J_H are not likely to vary much across the MIT, the self-consistent modification of hopping in a way consistent with (i) holds the key to increased itinerance. In any case, screening-induced renormalisation of U, U' will occur only after the system has undergone an insulator-metal transition,

and it is hard to understand how the transition itself can be "derived" by reducing U, U' in the PI phase.

B. Implications for theory

As discussed above, the effective one- (or two-band), $S=1/2$ Hubbard model has turned out to be an inadequate starting point for V_2O_3. It is instructive to put recent developments in terms of a three-orbital, $S=1$ modeling in proper context, viewed as a natural development of the earlier models.

The validity of the hitherto widely used $S=1/2$ Hubbard model used for 30 years to describe V_2O_3 rested on the following argument. Castellani *et al.*[9] started with a single c-axis V-V pair in the real crystal structure of V_2O_3, and solved the two-site cluster, including U, U' and J_H. They assumed that screening processes reduce the values of these parameters and, in particular, that $J_H \simeq 0.1U$. With this choice, and in the situation where the t_{2g} levels were split into an a_{1g} singlet and e_g^π doublet by the trigonal distortion, they found that the two electrons in the a_{1g} orbitals on the pair form a total spin singlet, while the second electron populates the E_g states (see Fig. 12 upper panel). The resulting model is clearly a $S=1/2$, two-orbital Hubbard model, with an orbital ordered, spin AF ground state. Based on this picture, the one-band Hubbard model was studied extensively for 20 years with a variety of techniques.[20] As is clear from the earlier discussion, a variety of recent results run into direct conflict with the one-band modeling.

Theoretically, the discrepancy has to do with the fact that J_H, which controls the spin state at each V site, is very poorly screened in a solid. This implies that J_H in V_2O_3 is larger than $0.1U$, the value used by Castellani *et al.*[9] Indeed, with $J_H > 0.2U$, the ground state has been found to have $S=1$, with a change to low-spin $S=0$ state as J_H is reduced toward the value used by Castellani *et al.*[9]

Given that the occupation of the a_{1g}, e_g^π orbitals changes discontinuously at the MIT, one would expect an important role for the trigonal field (since it acts like a fictitious external field in the orbital sector). This is expected to sensitively determine the occupancy of each orbital (orbital polarization) in much the same way as the magnetization of a paramagnet is a function of an applied magnetic field. In particular, one expects that the lower-lying (in the atomic picture) orbital state(s) should be more localized in the solid (e_g^π) in comparison to the higher-lying (a_{1g}) ones, as we shall, indeed, find to be the case. Furthermore, the fact that the ratio of the orbital occupations changes discontinuously at the MIT forces one to associate a corresponding change in the trigonal field as well.

A theoretical picture of the MIT in V_2O_3 must address these issues in a consistent way. Here, we focus our attention on the paramagnetic insulating and metallic states. The observation of strong correlation signatures in the paramagnetic phase of V_2O_3 as described above implies a fundamental inadequacy of the band description and mandates use of a strong correlation picture. Indeed, a consistent description of the PI/PM MIT requires a theoretically reliable description involving marriage of structural aspects (LDA) and strong correlation features (MO-DMFT).

In the rest of this paper, we confine ourselves to the theoretical description of the PI/PM Mott transition in V_2O_3. Starting with a detailed exposition of the LDA+DMFT(IPT), which we use as a solver (the pros and cons of using IPT vis-a-vis other impurity solvers will be discussed), we will derive a two-fluid description of the PI/PM transition in V_2O_3, attempting to achieve an internally consistent description. Finally, a quantitatively accurate description of the one-particle spectral function across the MIT *and* low-T thermodynamics will be demonstrated within this scenario.

III. LDA+DMFT TECHNIQUE

As argued in detail and shown in recent work,[21] LDA+DMFT has turned out to be *the* method of choice for a consistent theoretical description of the competition between quasi-atomic, strong Coulomb interactions (multiorbital) and itinerance (LDA spectra, encoding structural details in the one-electron picture) in real three-dimensional transition-metal and rare-earth compounds. The central difficulty in this regard has been the choice of an appropriate impurity solver to solve the multiorbital, asymmetric Anderson impurity problem. Two ways have been used with varying degrees of success: iterated perturbation theory (IPT) and quantum Monte Carlo (QMC). We should also specify that the noncrossing approximation (NCA) has also been used in this context.[22] As is known, it fails at low temperatures ($T < T_K$, the Kondo temperature) for the one-channel single-impurity Anderson model (SIAM), but it may be a good approximation to use in the multichannel SIAM. Finally, powerful numerical techniques, such as the numerical renormalization group (NRG)[23] and dynamical density-matrix renormalization group (D-DMRG),[24,25] have been used to study the one-band Hubbard model in $d=\infty$. These are extremely expensive numerically, effectively precluding their application to study real correlated systems (where the actual LDA band structure must be married to multiorbital DMFT).

We have used multiorbital (MO) extension of IPT to solve the impurity model. On the one hand, such an approach should be valid if the behavior of the multiorbital SIAM is *analytic* in U, U', J_H; this is known to hold for the general asymmetric version. MO-IPT also has the advantage of being extendable to $T=0$, and the self-energies can be extracted at modest numerical cost. On the other hand, it is by no means exact and calculations done for the one-band Hubbard model[21] show *quantitative* differences between IPT and QMC results for the critical value of $U=U_c$ at which the MIT occurs. It has also been claimed[26] that the IPT spectral functions are very different from the QMC ones, and the latter are claimed to be more reliable vis-a-vis the *true* spectral function, as well as with the actual, experimentally determined spectral functions. Here, we should emphasize that the IPT results for the many-body DOS are in excellent agreement with *both* exact diagonalization[24] as well as dynamical DMRG results for the one-band Hubbard model in $d=\infty$. Although no such evidence exists for multiorbital models, we believe that the above arguments show that IPT is a good approximation, even though it is not "numerically exact."

With these caveats, we describe our multiorbital iterated perturbation theory (MO-IPT) for multiband correlated systems. For early TM oxides, one-electron band-structure calculations show that, in three-dimensional cases, the t_{2g} DOS is well separated from the e_g DOS as well as from the O-2p DOS. More precisely, the "t_{2g}" DOS does have contributions from components of the e_g and O-2p orbitals having t_{2g} orbital symmetry. Structural effects, such as those produced by trigonal crystal fields (V_2O_3)[27] and antiferroelectric distortions (VO_2)[28] are adequately described by LDA. In addition, the multiorbital Coulomb interactions are parametrized by three parameters U, U', and J_H. The Hund's rule coupling, J_H, is very poorly screened and can be taken equal to its atomic value. The intraorbital (U) and interorbital (U') Coulomb interactions are screened in the actual solid: usually, their screened values have traditionally been calculated using constrained LDA. In correlated systems, this is a problem; however, as the dynamical processes screening these parameters arise from *correlated* electrons having dualistic (itinerant-localized) character, rather than from free band electrons. This well-known problem has received scant attention to date; indeed, we are aware of only one previous work attempting to cure this malady.[29] Below, we will show how the renormalized U, U' are self-consistently computed in a *correlated* approach and lead to a consistent description of the PES results in the PM phase.

A. Many-body Hamiltonian

Generally, the full many-body Hamiltonian for early TM oxides is written as

$$H = \sum_{\mathbf{k}ab\sigma} (\epsilon_{\mathbf{k}a} + \epsilon_a^0 \delta_{ab}) c^\dagger_{\mathbf{k}a\sigma} c_{\mathbf{k}b\sigma} + U \sum_{ia} n_{ia\uparrow} n_{ia\downarrow} + U' \sum_{ia \neq b} n_{ia} n_{ib} - J_H \sum_{ia \neq b} \mathbf{S}_{ia} \cdot \mathbf{S}_{ib}, \quad (1)$$

where $a, b = xy, yz, zx$ denote the three t_{2g} orbitals, U (U') the intraorbital (interorbital) Coulomb interaction term and J_H the Hund's rule coupling. Note that $U' = U - 2J_H$ couple the three t_{2g} orbitals, requiring a multiorbital LDA+DMFT description to treat these effects. Details of the actual one-electron band structure in the real lattice structure are encoded in the one-electron band dispersion $\epsilon_{\mathbf{k}a}$; the corresponding LDA DOS is $\rho(\omega) = N^{-1} \Sigma_{\mathbf{k}a} \delta(\omega - \epsilon_{\mathbf{k}a})$. Here $\epsilon_a^0 = \epsilon_a - U(n_{a\sigma'} - \frac{1}{2}) + (J_H/2)\sigma(n_{a\sigma} - 1)$, where ϵ_a are the on-site energies of t_{2g} orbitals within LDA and the rest of the terms are subtracted therefrom in order to avoid double counting of interactions already treated on the average by LDA.

With these qualitative remarks, we now describe our multiorbital LDA+DMFT procedure. We emphasize that the basic method was already developed in Ref. 21, and here, we extend this ideology using more detailed analysis to study the *full* one-electron spectral function in *both* insulating and metallic phases in V_2O_3. Our strategy is as follows.

(i) Beginning with LDA results in the real corundum lattice (see Fig. 4), derive a correlated Mott insulating state using multiorbital DMFT with $U = 5$ eV, and $U' = 3$ eV (we use $J_H = 1.0$ eV for V^{3+}), values obtained from constrained LDA. The LDA bandwidth is $W = 2.5$ eV, and the bare LDA trigonal field is read off as $\Delta = 0.32$ eV. In what follows, we will work in the basis of LDA eigenstates, which diagonalizes the one-particle density matrix.

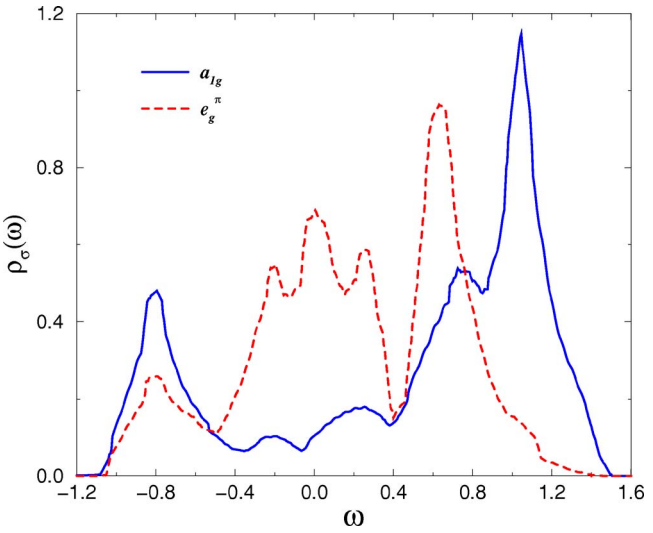

FIG. 4. (Color online) LDA partial density of states for the e_g^π (dashed red line) and a_{1g} (solid blue line) orbitals, obtained from Ref. 30.

(ii) Mimic the effects of external pressure by noting that it should lead to modification of the *renormalized* (correlated) value of the trigonal field. In line with this ideology, propounded previously by Mott and co-workers, we search for the instability of the correlated (Mott insulator) solution found in (i), to a second solution of the DMFT equations as a function of Δ. We emphasise here that we do *not* change the bare LDA parameters; indeed, we argue that a Mott transition from a correlated insulator to correlated metal *cannot* be validly described by changing bare LDA parameters, since these have no clear meaning in a strongly correlated system.

(iii) To provide a quantitative description of the one-electron spectral function in the metallic phase, we use the correlated (DMFT) results to compute the screening-induced reduction in U, U' *in* the metallic phase. This is crucial: we derive the screened U, U' in the PM phase *after* deriving the I-M transition and do not derive the I-M transition itself by reducing U, U', as seemingly done in earlier work.[21,30] Using the DMFT result, the screened U, U' are estimated by an extension of Kanamori's t-matrix calculation to finite density.

Using the screened values of U, U' (note that J_H is almost unaffected by screening, so we use the same value for it throughout), we compare our theoretical (correlated) DOS to PES and x-ray-absorption spectroscopy (XAS) results obtained experimentally in the PM phase.

Incorporation of electron correlations into the LDA gives rise to a two-stage renormalization. In stage 1, U, U', and J_H give rise to multiorbital Hartree shifts in the on-site orbital energies of each t_{2g} orbital. In V_2O_3, the trigonal field splits the t_{2g} degeneracy, with the lowest a_{1g} orbital [$\simeq (xy + yz + zx)$] lying about $\Delta = 0.32$ eV below the higher lying e_g^π or-

bitals $[\simeq(xy-yz),(2xy-yz-zx)]$ within LDA. Given this, the a_{1g} orbital is always occupied by one electron, the second residing in the e_g^π orbitals. The observation of $S=1$ on each V site requires strong J_H, implying even stronger U, U', even in the PM phase.

Multiorbital Hartree shifts renormalize the orbital energies: $\epsilon_{a_{1g}}=\epsilon_0+U'n_{e_g^\pi}$ ($\epsilon_{e_g^\pi}=\epsilon_0+\Delta+U'n_{a_{1g}}$), where $n_{e_g^\pi}$ ($n_{a_{1g}}$) is the e_g^π (a_{1g}) orbital occupation. These shifts correspond to effects captured by LDA+U.[31] They do give the correct, insulating ground states (with orbital and/or magnetic order), but *cannot* describe the phase transition(s) from correlated Mott insulators to correlated metals. This can be traced back to the fact that LDA+U treats correlations on a static level, neglecting *quantum* nature of electron dynamics and, thus, cannot access the spectral weight transfer-driven physics at the heart of Mott-Hubbard transitions.

Stage 2, in a one-electron picture, this would be the end of the story. In reality, however, hopping of an electron from a given site to its neighbor(s) is accompanied by *dynamical* generation of particle-hole pairs (the more, the larger U, U' are), which inhibit its free band motion. Electrons can move quasi-coherently by dragging their corresponding "electronic polarization cloud" along. With increasing U, U', electrons get more and more "localized," corresponding to transfer of coherent low-energy spectral weight to high-energy (quasiatomic) incoherent regions, until at the MIT, *all* the weight resides in the incoherent Mott-Hubbard bands. It is precisely this effect that is out of scope of LDA+U and requires dynamical mean-field theory (DMFT) for a consistent resolution.

Since the system is strongly correlated, the small changes in bare LDA parameters caused by stage 1 lead to large changes in transfer of dynamical spectral weight. Specifically, in systems undergoing MIT, small changes in bare LDA values of lattice distortion(s) transfer high-energy spectral weight to low energies, driving the Mott transition.

B. One-particle Green's functions

Given the actual LDA DOS for the t_{2g} orbitals (this includes the V-d orbitals and O $2p$ part having "t_{2g}" symmetry), the band Green's functions within the LDA (in the basis that diagonalizes the one-particle density matrix) are $G_{ab}(\omega)=\delta_{ab}G_a(\omega)=\delta_{ab}(1/N)\Sigma_{\mathbf{k}}(\omega-\epsilon_{\mathbf{k}a})^{-1}$. We define the correlated one-electron Green's function and the associated irreducible self-energy for each orbital a, by $G_{a\sigma}(\omega)$ and $\Sigma_{a\sigma}(\omega)$; the two are related by the usual Dyson's equation,

$$G_a^{-1}(\omega)=[G_a^0(\omega)]^{-1}-\Sigma_a(\omega). \tag{2}$$

It is obvious that the Green's functions can be exactly written down for the noninteracting case, as well as for the atomic limit ($\epsilon_{\mathbf{k}a}=0$). In contrast to the case of the one-band Hubbard model, however, the exactly soluble atomic limit contains the local, interorbital correlation function, $\langle n_a n_b\rangle$, in addition to $\langle n_a\rangle$.

1. MO-IPT: An interpolative ansatz for multiorbital systems

In the spirit of the IPT developed by Rosenberg[32] for the one-orbital Hubbard case, we require an interpolative scheme that connects the two exactly soluble cases above and gives correlated Fermi-liquid behavior in the metallic phase, and a Mott-Hubbard transition from a correlated FL metal to a Mott insulator as a function of U, U' for commensurate cases. In order to achieve this, we have extended the philosophy of Ref. 33.

The central requirements for a consistent interpolative scheme capable of describing all of the above are that (i) the one-electron Green's function,

$$G_a(\omega)=\frac{1}{N}\sum_{\mathbf{k}}\frac{1}{\omega+\mu-\Sigma_a(\omega)-\epsilon_{\mathbf{k}a}}, \tag{3}$$

where $\epsilon_{\mathbf{k}a}$ describes the dispersion of the LDA bands for orbitals $a,b=t_{2g}$, and the self-energy is given by

$$\Sigma_a(\omega)=\frac{\sum_b A_{ab}\Sigma_{ab}^{(2)}(\omega)}{1-\sum_b B_{ab}\Sigma_{ab}^{(2)}(\omega)}, \tag{4}$$

with

$$\Sigma_{ab}^{(2)}(\omega)=N_{ab}\frac{U_{ab}^2}{\beta^2}\sum_{lm}G_a^0(i\omega_l)G_b^0(i\omega_m)G_b^0(i\omega_l+i\omega_m-i\omega) \tag{5}$$

being the second-order (in U, U') contribution. Here, $N_{ab}=2$ for $a,b=e_{g1}^\pi,e_{g2}^\pi$ and 4 for $a,b=a_{1g},e_{g1,2}^\pi$. Finally, the bath propagator is given as

$$G_a^0(\omega)=\frac{1}{\omega+\mu_a-\Delta_a(\omega)}, \tag{6}$$

with $\Delta_a(\omega)$ interpreted as the dynamical Weiss field for orbital a. (ii) the interpolative self-energy for each orbital a should be chosen by fixing interpolative parameters such that the exact Friedel-Luttinger sum rule is strictly (numerically) obeyed, and, (iii) to reproduce the Mott insulator beyond a critical coupling, a high-energy expansion around the atomic limit is performed, yielding another equation for the interploative parameters. Here, the high-energy expansion is truncated by including only the first few terms, which guarantee the exact reproduction of the first three moments of the one-electron spectral function. In contrast to the one-band case, however, the exact atomic limit for the multiorbital case contains the local, interorbital correlation function, $D_{ab}[n]=\langle n_a n_b\rangle$.[34] We are aware of only one earlier work[33] where $D_{ab}[n]$ is computed using the coherent potential approximation (CPA). Strictly speaking, this is an approximation to the Hubbard model(s), which is qualitatively valid in the Mott insulating state, but is known to fail in the correlated PM phase(s). This is because CPA replaces the actual, dynamical (annealed) "disorder" in the PM phase(s) by quenched static disorder and, thus, fails to capture the dynamical Kondo screening central to deriving correct (correlated) FL behavior in the PM phase. Given this, it is hard to identify the extent to which computed results depend on introducing such approximations, and this should be checked carefully by comparison to calculations that compute all local correlators in a single, consistent scheme. The correct way to compute

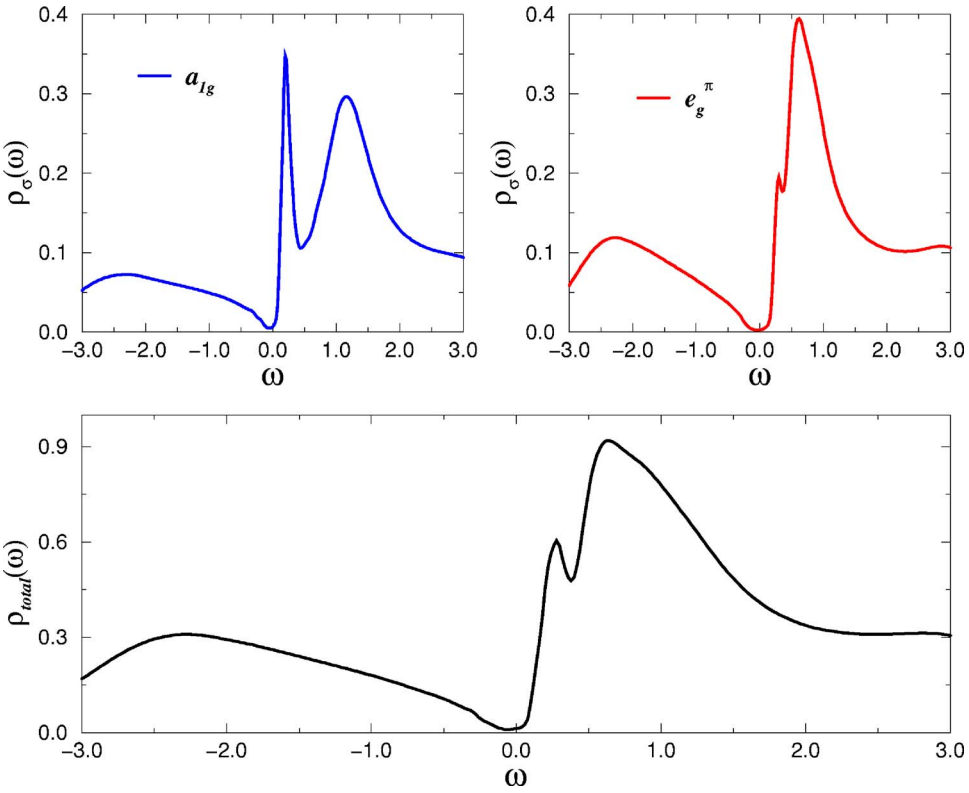

FIG. 5. (Color online) Orbital-resolved (upper panels) and total (lower panel) one electron spectral function for the insulating phase of V_2O_3 obtained with 5.0 eV and $J_H=1.0$ eV.

$D_{ab}[n]$ is actually not complicated within multiorbital IPT and is described below.

These two equations for the parameters A_{ab} and B_{ab} are solved to yield these as explicit functions of U, U', $\langle n_a\rangle$, $\langle n_a n_b\rangle$, and $\langle n_a^0\rangle$ [this last average is the "effective" number of fermions in orbital a corresponding to an effective Green's function used in the interpolative IPT (see Refs. 33 and 35)]. Explicitly, we have

$$A_{ab} = \frac{n_a(1-2n_a) + D_{ab}[n]}{n_a^0(1-n_a^0)} \tag{7}$$

and

$$B_{ab} = \frac{(1-2n_a)U_{ab} + \mu - \mu_a}{U_{ab}^2 n_a^0(1-n_a^0)}, \tag{8}$$

where n_a and n_a^0 are defined from the GFs $G_a(\omega)$ and $G_a^0(\omega)$. The interorbital correlation function $D_{ab}[n]$ is calculated from

$$D_{ab}[n] = \langle n_a\rangle\langle n_b\rangle + \frac{1}{U_{ab}}\int_{-\infty}^{+\infty} \Xi(\omega) f(\omega) d\omega, \tag{9}$$

the last term following from the equation of motion for $G_a(\omega)$ and $\Xi(\omega) \equiv -1/\pi\, \mathrm{Im}[\Sigma_a(\omega)G_a(\omega)]$.

The above equations form a closed set of coupled, nonlinear equations, which are solved numerically. We found fast convergence of the self-consistent system of equations, and typically 20 iterations sufficed for the parameter values considered here. The converged results allow us to study the one-particle DOS and the corresponding orbital occupations, spin states, as well as the strength and character of local multiorbital correlations in *both* PI and PM phases, as described below, in detail.

IV. RESULTS AND DISCUSSION

In this section, we present a detailed set of results for the one-particle spectral function in *both* the PI and PM phases in V_2O_3. While doing so, we will make extensive contact and discuss important differences between our work here and previous results recently obtained by other authors.[21,30]

In Fig. 5, we show the single-particle DOS for the Mott insulator, obtained with $U=5.0$ eV, $U'=3.0$ eV, and $J_H=1.0$ eV as correlation parameters for this system. These are slightly different from those used in our previous work,[27] but are roughly the same as those used by Held *et al.*[30] A clear Mott-Hubbard gap, $E_G=0.2$ eV, is seen, and, as expected from the orbital assignment, the e_g^π states are more localized in the solid. The renormalized trigonal field $\Delta_t^r = \delta_{a_{1g}} - \delta_{e_g^\pi} = 0.32$ eV, is read off directly from Fig. 5. The orbital occupations are computed to be $(n_{a_{1g}}, n_{e_{g1}^\pi}, n_{e_{g2}^\pi} = 0.32, 0.34, 0.34)$ in the PI, in nice agreement with XAS estimations.

We now study the paramagnetic metallic state obtained as an instability of the correlated Mott insulator derived above. In other works, the PM state is "derived" not by searching for an instability of the correlated PI state under pressure, but by computing the LDA band structure for the "metallic" state *without* correlations. The screened values of U, U' are computed using constrained LDA, and these are then used to describe the PM phase. In reality, however, one has to study the transition to the PM phase without leaving the correlated picture, and derive the transition by searching for the second, metallic solution of the DMFT equations under pressure.

To justify our approach, we specify the problems associated with earlier approaches.[21,30,36] First, it is theoretically inconsistent to derive a phase transition between two strongly correlated phases by using corresponding LDA band structures to separately derive the two phases. This is because using changes in bare LDA parameters to study correlated phases is clearly problematic, since these parameters have no clear meaning in a correlated picture. One must use the *renormalized* values of these parameters instead, and these are generically modified in unknown ways by strong multiorbital correlations. These changes in bare LDA parameters, and the modification of the response of correlated electrons to these changes, must be selfconsistently derived *within* the LDA+DMFT procedure. Clearly, this route has not been used in other approaches.

Second, follows that an inescapable consequence of using such approaches is that the values of U, U' used for the PM phase are computed using constrained LDA (i.e., using the uncorrelated band structure, assuming that the screening electrons are *free* band electrons). However, in reality, the screening electrons in the correlated PM phase have a dualistic character generic to the Mott-Hubbard character of the system. As is known from Ref. 20, the electronic kinetic energy, or itinerance, is reduced in the PM phase; it is these correlated electrons that screen U, U' in the real correlated system. In an *ab initio* treatment, the effective U, U' should be computed using the *correlated* spectral functions to estimate screening. Replacement of the renormalized spectral functions by bare LDA ones will introduce an approximation, overestimating the screening of U, U' (this is hard to quantify, but is estimated to be of order of 20%).

In order to avoid these difficulties, we adopt the following strategy. (i) We hypothesise that external pressure modifies the trigonal field. To our knowledge, this is not completely new: Mott and co-workers proposed such ideas in the 1970s,[1] and more recently, Tanaka made a similar hypothesis in a cluster approach for V_2O_3.[37] To model this change in Δ_t under pressure, we *do not* change the trigonal field by hand. Rather, we input trial values of Δ_t, changing it from its value in the (Mott) PI by small trial amounts, and *search* numerically for its critical value, Δ_t^c, which stabilizes the second, correlated metallic solution of the DMFT equations. The new values of Δ_t in the (correlated) PM phase are again read off from the converged DOS for each orbital. We emphasize that we do not decrease U, U' by hand, neither do we use different LDA DOS for different phases, for reasons explained before. We note that Savrasov *et al.*[38] have employed similar ideology to study the giant volume collapse across the $\alpha-\delta$ transition in *Pu*.

In a strongly correlated system, small changes in the *renormalized* trigonal field lead to large changes in dynamical spectral weight transfer from high-to low energies, typically over a scale of a few electron volts. This is precisely our mechanism for the first-order Mott transition in V_2O_3 under pressure. We expect the free energy to have a double-well structure. Pressure changes the trigonal field (we remind the reader that Δ_t acts like an external field in the orbital sector), lowering the second minimum (PM) relative to the first (PI) beyond Δ_t^c.

(ii) Using the converged DOS for each orbital, the occupation(s) of various orbitals (and their changes from their PI values), the local spin value at each V site, and information about the detailed character of the PM state is directly obtained.

In Fig. 6, we show our results for the PM phase obtained within our technique. At $T=0$, the hypothetical PM phase (it is never observed in reality) shows a sharp, quasi-coherent FL resonance. We identify this feature with combined spin-orbital Kondo screening in the PM phase of a multiorbital Hubbard model. This is easily seen as follows. To obtain a correlated Mott insulator, we need not only $U=5.0$ eV, but also $U' \simeq (U-2J_H)=3.0$ eV; indeed, if U' were ignored, a t_{2g} electron hopping from one V site to its neighbor could always hop off like a band electron just by going into an unoccupied t_{2g} orbital at that site, making a PI state impossible. Given the small spectral weight carried by this feature, we expect a low-lattice coherence scale, above which the PM would be described as an incoherent metal. The trigonal field in the PM, $\Delta_t'=-0.291$ eV and the occupations of each t_{2g} orbitals, $[n_{a_{1g}}, n_{e_{g1}^{\pi}}, n_{e_{g2}^{\pi}}=0.38, 0.31, 0.31]$, are read off from the converged PM solution of the DMF equations. Very satisfyingly, the spin state remains unchanged, and the orbital occupations change across the MIT in semiquantitative agreement with XAS results.[11] We note that these numbers are slightly different from those derived in our earlier work. This difference is a direct consequence of our use of a reduced U in the present work [note that $U=6.0$ eV) was used in our earlier work].

In Figs. 7 and 8, we show the effect of finite temperature on our results. As expected on general grounds within the DMFT framework, the FL resonance is broadened by finite-T and lowered in height (the pinning of the interacting DOS at E_F to its LDA value, dictated by Luttinger's theorem, holds only at $T=0$). In agreement with very recent observations,[16] we indeed observe a broadened "quasiparticle" in the PM, and closing in of the Mott gap in the PI by incoherent spectral weight transferred across large energy scales from high to low energies. As observed by Allen,[39] this implies that there is no fundamental difference between the "metal" and "insulator" at sufficiently high T; this agrees with the observation that the first-order Mott transition is replaced by a smooth crossover at high T.

The effects of introducing chemical disorder is modeled by adding an on-site term $H_{\rm dis}=\Sigma_{ia\sigma} v_i n_{ia\sigma}$ to H [Eq. (1)].[40] We consider binary alloy distribution for the ionic energies (v_i), which are distributed according the probability density $P(v)=(1-x)\delta(v)+x\delta(v-\nu)$. Here, x is the concetration of the M-ion and ν is the energy difference between the vanadium on-site energy (ϵ_a^0) with respect to the M ionic energy. Our results for $x=0.038$ and two values of disorder potential ν in the PM ($U=5$ eV) phase are shown in Fig. 9. These results are obtained by combining multiorbital IPT with the coherent-potential approximation (CPA).[41] Comparing Figs. 7 and 8 to Fig. 9, it is clear that, at sufficiently high-T, the spectra in the chemically disordered PM and those nondisordered PI (Fig. 7) and PM (Fig. 8) phases do resemble each other qualitatively.

An extremely important conclusion follows directly from an examination of the orbital-resolved DOS in the PM phase. We find that the e_g^{π} orbital DOS shows "Mott-insulating"

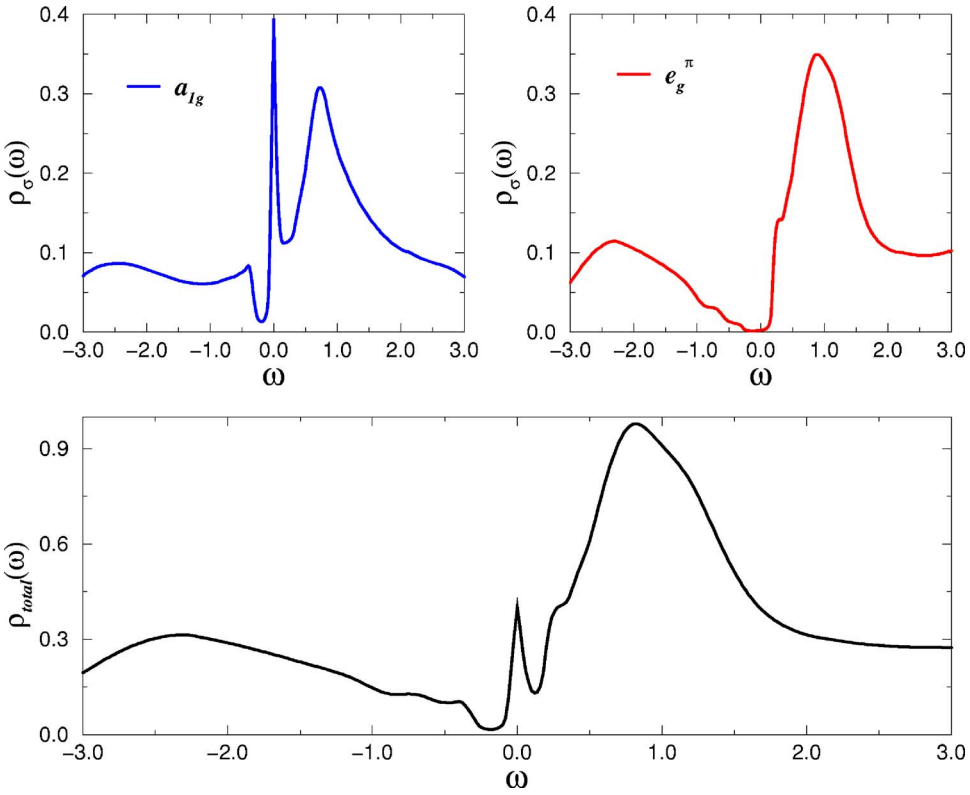

FIG. 6. (Color online) Orbital-resolved (upper panels) and total (lower panel) one-electron spectral functions for the metallic phase of V_2O_3. Note that only the a_{1g}-orbital DOS crosses E_F in the metallic phase; the e_g^π orbitals still shows Mott-Hubbard insulating features, showing the "two-fluid" character of the MIT in V_2O_3.

(see Fig. 6) behavior, while only the a_{1g} orbital DOS is responsible for the metallicity. This constitutes an explicit realisation of the "two-fluid" model used phenomenologically in connection with the MIT in disordered semiconductors in the past.[1] In Refs. 27 and 28, we already showed the orbital selective character, as well as the evolution of the DOS at E_F as a function of the occupation of the a_{1g} orbital.

A clear first-order I-M transition around $n_{a_{1g}}=0.38$ was found, involving, as described above, a discontinuous change in (self-consistently determined) occupations of each orbital. These observations are intimately linked to the multiorbital Mott-Hubbard character of correlations in V_2O_3. Polarized

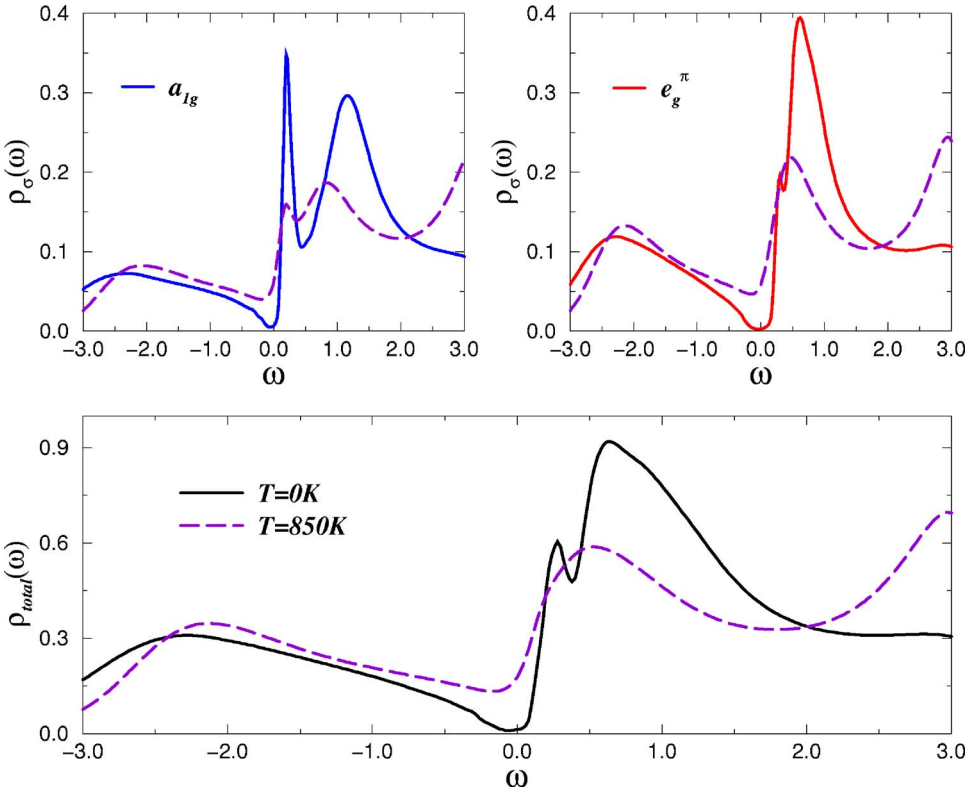

FIG. 7. (Color online) Effect of temperature T on the orbital-resolved (upper panel) and total (lower panel) one electron spectral functions for the insulating phase of V_2O_3.

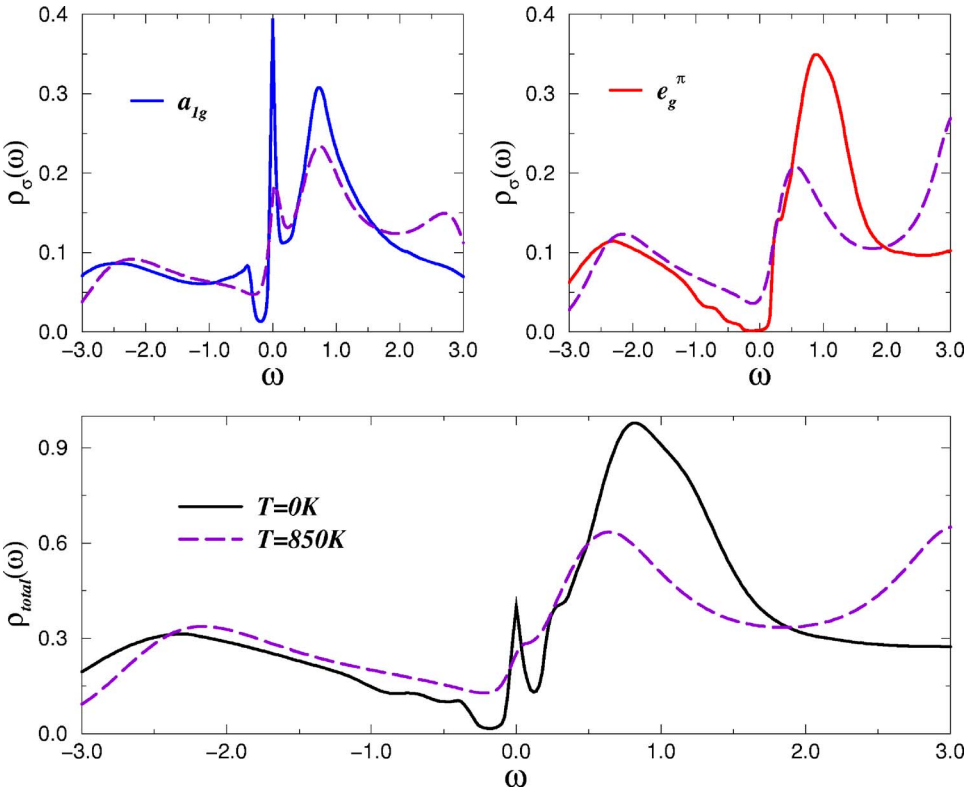

FIG. 8. (Color online) Effect of temperature T on the orbital-resolved (upper panels) and total (lower panel) one electron spectral functions for the metallic phase of V_2O_3.

XAS results might already hold the clue to establishing an approximate two-fluid character of the PM phase: the a_{1g} spectral weight should dominate over the e_g^π contribution for energies up to the Mott gap. Orbital resolved optical studies could also be used to test our picture.

Strong indirect support for our picture comes from the early observation[10] of an anisotropic change in the lattice constants along a/b (planar) and c axes across the P-MIT in V_2O_3. Instead of a uniform volume collapse expected across the MIT,[42] increase in $a(b)$ and a *decrease* in c was found

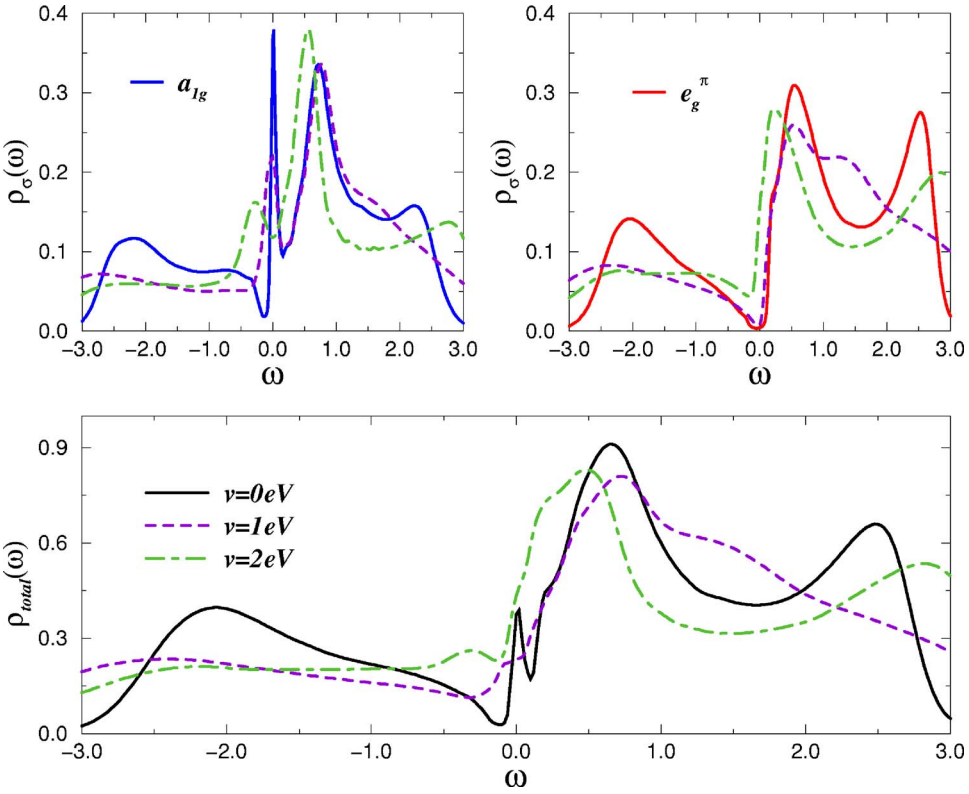

FIG. 9. (Color online) Effect of disorder (v) with a binary-alloy distribution on the orbital-resolved (upper panels) and total (lower panel) one-electron spectral functions for the metallic phase of V_2O_3.

across the MIT. Such an anisotropic volume change across the MIT is inconsistent with *simultaneous* gapping of all t_{2g} orbitals (where we would expect an isotropic volume change), but is completely consistent with our (orbital selective) two-fluid picture derived above.

A. Comparison with PES and XAS

In this section, we describe how our approach provides an excellent description of the experimental photoemission spectroscopy (PES) and x-ray-absorption spectroscopy (XAS) data on V_2O_3 in the PM phase. As argued before, this requires us to recompute the full one-particle local spectral function (total DOS) using values of U, U' renormalized by dynamical metallic screening in the *correlated* metallic phase. In order to do this, we have used an extension of Kanamori's t-matrix approach[3] to estimate these parameters.

In the multiorbital case, this is a horrendous problem, in general. Fortunately, in the effective two-fluid picture of the PM phase derived above, the general analysis can be simplified. This is because the e_g^π electrons remain "insulating" (i.e., Mott localized, up to energies of the order of the Mott-Hubbard gap). We then expect only the a_{1g} electrons to provide efficient screening and therefore, consider only the a_{1g} band in the computation of the effective U, U' below. In general, we need the full **q**-dependent particle-particle susceptibility for this purpose. Using the LDA+DMFT Green's function for the a_{1g} orbital,

$$\chi_{pp}(\mathbf{q}) = -\frac{1}{N}\sum_{nm\mathbf{k}} G_{a_{1g}}(\mathbf{q}-\mathbf{k}, i\omega_m - i\nu_n) G_{a_{1g}}(\mathbf{k}, i\nu_n). \tag{10}$$

In $d=\infty$, this can be expressed as an integral over the LDA DOS and the full irreducible one-electron self-energy,[20] permitting a direct evaluation. The onsite Hubbard U is renormalized by the local part of this susceptibility via

$$U_{\text{eff}} = \frac{U}{1 + U\chi'_{\text{loc}}(\omega)}. \tag{11}$$

Using the relation $U \simeq (U' + 2J_H)$, valid for t_{2g} systems, along with the fact that J_H is essentially unscreened, we estimate U, U' in the PM phase. We observe that this implies a frequency-dependent $U_{\text{eff}} = U(\omega)$. We have found, however, on computation that the ω dependence is weak for energies up to the Mott gap and, thus, we use its $\omega=0$ value $U_{\text{eff}} = U(0)$ in what follows.

Starting with the values of U, U' used earlier, we estimate $\chi'_{\text{loc}}(0) \simeq 0.084$, yielding $U_{\text{eff}} \simeq 3.5$ eV. With $J_H = 1.0$ eV, this implies that $U' \simeq 1.5$ eV. We have recomputed the one-electron spectral function for the PM phase using these values. Because of the reduction of U, U' as above, the t_{2g} orbital occupation is now $(n_{a1g}, n^\pi_{eg1}, n^\pi_{eg2}) = (0.36, 0.32, 0.32)$, in even better agreement with XAS results.[11]

Our results for $U=3.5$ eV are compared to experimental work[14,15,43] in Fig. 10. Very satisfyingly, excellent quantitative agreement over almost the whole energy scale from $-3.0 \leqslant \omega \leqslant 1.2$ eV is clearly observed. In addition to the detailed shape of the lower Hubbard band (in PES), excellent agreement with the intense peak in XAS is also clear. Consideration of parts of the spectrum for $\omega \leqslant -3.0$ eV and $\omega \geqslant 1.2$ eV is hampered by our restriction to the t_{2g} sector in the LDA+DMFT calculations.

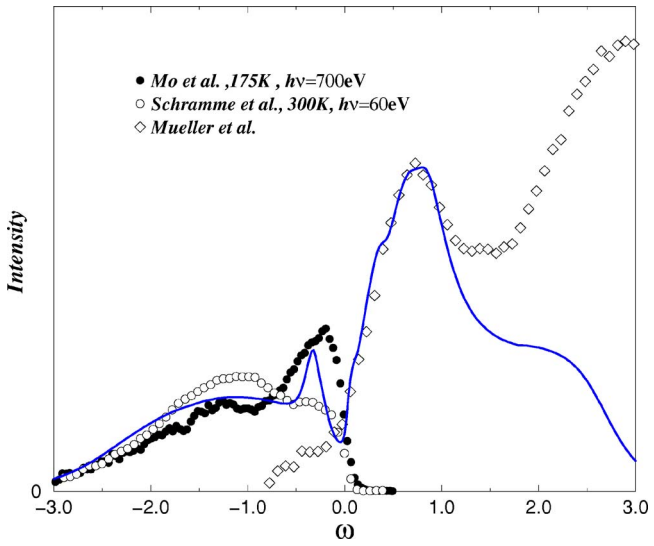

FIG. 10. (Color online) Comparison of theoretical LDA+DMFT result (solid blue line) for the total one-electron spectral function in the metallic phase of V_2O_3 to the experimental results taken from Refs. 14 and 15 (for PES) and from Ref. 43 (for XAS).

However, though good, the agreement is not quite as perfect in the low-energy region; our computed "broad" peak (ascribed to a "quasiparticle" in earlier work[15]) is narrower than the experimental feature by a factor of 1.8. On first sight, this might seem to confirm the interpretation in the earlier work. However, we observe that this feature is peaked at $\omega=-0.37$ eV, while a clear pseudo-gap-like dip is resolved around E_F. Hence, in our picture, the metallic phase cannot be described in a FL quasiparticle language; instead, short-lived, incoherent, non-FL pseudoparticles should dominate the PM phase. Interestingly, observation of a linear-in-T (instead of the T^2 form for a correlated FL) resistivity supports a non-FL quasiparticle interpetation. It is possible that the T regime where this is valid lies *above* an effective FL coherence scale (below which a T^2 term in resistivity would follow), which is masked by emergence of orbital and/or spin-ordered insulating states at lower T. At $T > T_{\text{coh}}$, the dc resistivity is indeed linear in T in a Hubbard model framework, where it arises from inelastic scattering off unquenched spin-orbital local moments in a $d=\infty$ multiband Hubbard model.

A comparison with the LDA+DMFT(QMC) work of Held *et al.*[30] is in order here. In Fig. 11, we compare our result to that of Held *et al.* relative to the recent PES result of Mo *et al.*[15] Clearly, the detailed shape of the lower Hubbard band is better reproduced by our result. At lower energies (above −0.3 eV), we find a pseudogap feature around E_F, instead of a FL quasiparticle found by Held *et al.* We draw attention to the fact that if the QMC calculation could (hypothetically) be done at $T=175$ K, corresponding to the experimental case, the QMC spectral function would show a

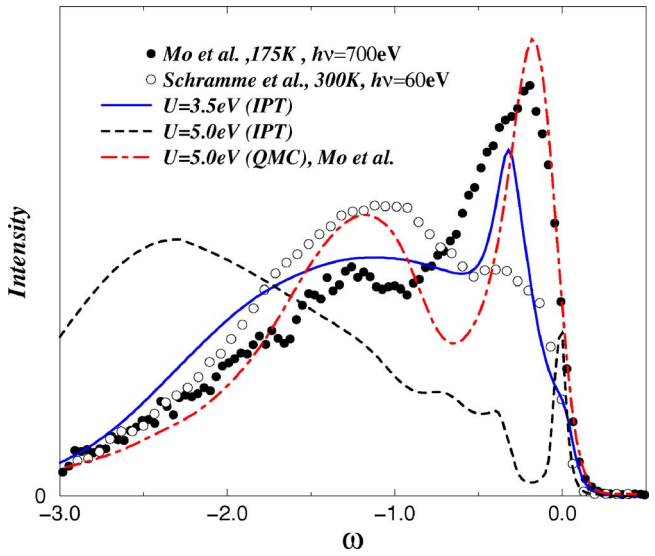

FIG. 11. (Color online) Comparison of two different LDA+DMFT results for the total one-electron spectral function in the metallic phase of V_2O_3 to the experimental results of PES taken from Refs. 14 and 15. The LDA+DMFT(QMC) result is taken from Ref. 16.

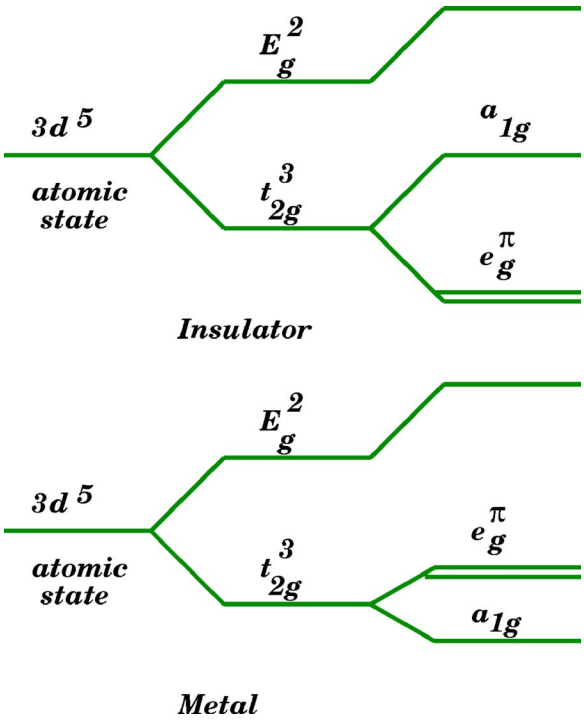

FIG. 12. (Color online) Schematic energy splitting of the $3d$ manifold in the PI (upper panel) and PM (lower panel) phases of V_2O_3. The correspondig t_{2g} orbital occupation is $(n_{a_{1g}}, n_{e^{\pi}_{g1,2}} = 0.32, 0.34)_{\mathrm{PI}}$ and $(n_{a_{1g}}, n_{e^{\pi}_{g1,2}} = 0.36, 0.32)_{\mathrm{PM}}$. The renormalized values of the trigonal field are $\Delta_{\mathrm{PI}} = 0.32$ eV and $\Delta_{\mathrm{PM}} = -0.003$ eV.

higher, narrower low-energy resonance than the one presented for $T = 300$ K by Held *et al.* Furthermore, the minimum between the central resonance and the lower Hubbard band would become deeper, and the Hubbard satellite would sharpen up, further deviating from the observed line shape. As it stands, the theoretical peak is narrower by a factor of two vis-a-vis experiment in the QMC work; this factor would increase with decreasing T in the QMC work. In contrast, our calculation (done at $T = 175$ K) shows an incoherent pseudogap feature at E_F with a peak centered around -0.31 eV. The calculated width of this peak is narrower than the experimental one by a factor of two, and it is only in this respect that LDA+DMFT(IPT) and LDA+DMFT(QMC) agree. In every other respect, there are noteworthy differences. Our results indicate that the PM phase is a non-FL metal, and the physical response should be dictated by incoherent, short-lived pseudoparticles. The QMC picture forces one to have to deal with FL-like quasiparticles even at $T = 300$ K. Very interestingly, the observation of an almost linear-in-T resistivity starting from T much lower than 300 K is completely consistent with our results and discounts the FL quasiparticle interpretation. Additionally, observation of strongly non-FL features in magnetotransport at low-T in V_2O_{3-y} suggests nonquasiparticle dynamics persisting to much lower T and implies that the FL quasiparticle picture would not take over below the lattice coherence scale, T_{coh}, as one would generically expect in a $d = \infty$ description. Unfortunately, it is impossible to study the evolution of the non-FL description to lower T in the region close to the PI-PM boundary because AF order preempts the (Mott) critical region as T is lowered.

Additional comparisons to more recent LDA+DMFT(QMC) work[44,45] is also in order. A comparison of our work with this calculation necessarily involves a restriction to the region $-2.0\ \mathrm{eV} < \omega < 1.5\ \mathrm{eV}$, since only t_{2g}-orbital DOS is included in our LDA+DMFT calculations. In this more recent work, the authors also compare their LDA+DMFT result for the unoccupied DOS to XAS measurements. Once again, a direct comparison of our result to theirs clearly shows that we obtain much better agreement with the XAS spectrum. Furthermore, a hypothetical QMC calculation done for $T = 175$ K would yield a much sharper central resonance, deviating even more from the observed XAS line shape. In our picture, the suppression of the XAS intensity near E_F and its rise with $\omega > E_F$ are both naturally understood as resulting from the low-energy pseudogap (as derived above) in the PM phase. To obtain some semblance of agreement with the experimental results, an unphysically large lifetime broadening, $\Delta\omega = 0.2$ eV (Ref. 45) is required in the LDA+DMFT(QMC) work.

In our calculation, the carrier lifetime is intrinsically large due to strong scattering between itinerant a_{1g} and localized e_g^{π} electrons, obviating the necessity to introduce such strong broadening "by hand." A very recent XAS study[46] of the local structure of V_2O_3 across the AFI-PM MIT clearly confirms our original hypothesis, wherein pressure is hypothesized to change the trigonal field splitting. In a correlated picture, the small changes in the renormalized trigonal field causes large changes in spectral weight transfer, driving the (first-order) Mott transition accompanied by changes in orbital occupation, exactly as observed in this XAS work.

B. Non-FL nature of the PM phase

To understand the origin of the observed non-FL features, we examine the metallic solution of the DMFT equations in

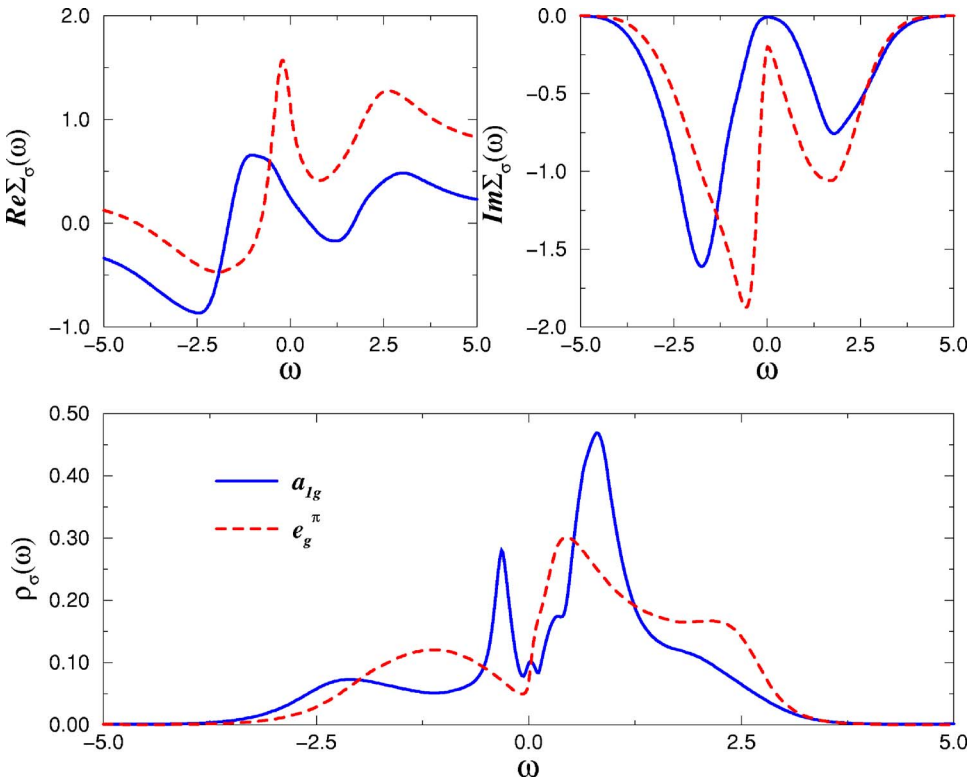

FIG. 13. (Color online) Orbital resolved self-energies (uper panels) and one-electron spectral function for the metallic phase of V_2O_3 for $U=3.5$ eV and $J_H=1$ eV.

more detail. The renormalized trigonal field splittings in the PI and PM phases are shown in Fig. 12. We draw attention to the fact that the e_g^π orbitals are almost perfectly degenerate in the PM phase. In $d=\infty$, and without symmetry breaking, this would lead to soft (zero-energy) interorbital electronic excitations. Self-consistent coupling of the itinerant carriers to these soft modes leads to the observed breakdown of the FL picture in the PM. In Fig. 13, we show the orbital resolved self-energies for the a_{1g}, e_g^π orbitals for the PM phase. Interestingly, while $\Sigma_{a_{1g}}(\omega)$ is FL-like around E_F, the self-energy for e_g^π orbitals, $\Sigma_{e_g^\pi}(\omega)$, has a distinct non-FL energy dependence, corresponding to a pseudogapped spectral function, $\rho_{e_g^\pi}(\omega)$.

In our two-fluid picture, mutual (strong) scattering between the itinerant (a_{1g}) and localized (e_g^π) electrons gives rise to a low-energy pseudogap in the spectral function in a way reminiscent of what happens in the Falicov-Kimball model in $d=\infty$,[20] destroying Landau FL quasiparticles and generating an incoherent metal phase and providing a natural explanation of the almost linear-in-T resistivity observed in the PM phase (arising from strong scattering between itinerant and localized parts of the full spectral function). An important aspect worth noting is that we have derived an effective Falicov-Kimball-like picture from an *ab initio* (LDA+DMFT) starting point. A very interesting issue in this connection pertains to the determination of the set of conditions (on the microscopic model) favoring the orbital selective Mott transition. Although this issue has received a lot of attention recently in connection with model Hamiltonians,[47,48] study of the necessary conditions in *real* systems remains a completely open problem.

Our work reveals a mechanism for the OSMT (orbital selective Mott transition) in real systems. Specifically, our results indicate that, in a correlated system with strong orbital-dependent (directional) one-electron hopping, strong multiorbital Coulomb interactions in the real crystal structure(s) might generically produce an OSMT via orbital selective changes in dynamical spectral weight transfer in response to small structural changes (variation in trigonal field under pressure in V_2O_3). Earlier LDA+DMFT work on Ca_2RuO_4 (Ref. 49) also finds an OSMT; all these conditions also hold there. We emphasize that the important role of structural changes in a strongly correlated situation, self-consistently modifying both the electronic spectrum and the lattice structure itself, has not hitherto been investigated as a source for OSMT. Our results here also represent a mechanism for an OSMT in real TMO systems. There is no compelling reason to associate this mechanism with V_2O_3; indeed, we expect it to be more widespread in multiorbital correlated systems undergoing Mott (I-M) transitions under external perturbations.

Additionally, the strong bonding-antibonding splitting observed in LDA results (see Fig. 4) further aids the generation of the observed pseudogap. This is a direct consequence of strong hopping along the a_{1g} orbitals, leading to strong covalency and robust singlet character between V-V pairs along the c axis (see Ref. 50 for an early discussion on this point). Our analysis does partially show up the effects of strong covalency, manifested in the pseudogap feature found above. However, the fact that we can resolve most of the spectrum accurately, but fail to reproduce the correct broadening of the low-energy feature, implies that it may be necessary to explicitly consider the dynamical effects of intersite (V-V) correlations for a complete resolution of the PES spectrum, as alluded to in Sec. II. This is, however, out of scope of LDA+DMFT and requires a cluster extension.

V. CONCLUSION

In conclusion, we have studied the first-order Mott transition under pressure in V_2O_3 using the state-of-the-art LDA+DMFT technique. We have proposed an orbital selective picture for the MIT, which is driven by large changes in the transfer of dynamical spectral weight (via DMFT) accompanying small changes in the renormalized trigonal field splitting under pressure. This is a characteristic signature of the dynamical effects of strong, multiorbital Coulomb interactions, and hence, the Mott transition is of the correlation-driven type. Very good quantitative agreement with the orbital occupations, spin state of V^{3+} ions, as well as effective mass enhancement in the PM state is obtained in both PI and PM phases. The MIT is found to be first order and orbital selective (only the a_{1g} DOS shows metallic behavior). Finally, using the correlated solution, we have computed the screening-induced renormalization of U, U' in the PM phase. Using these, excellent quantitative agreement with the full one-particle spectral function (PES *and* XAS) is found in the PM phase. These findings constitute strong support for our underlying two-fluid picture (orbital selective mechanism) found in our previous work,[27] which is ultimately an interesting manifestation of strong, multiorbital Coulomb interactions in this early transition-metal oxide.

ACKNOWLEDGMENTS

The authors would like to acknowledge H. Tjeng for valuable discussions. The work of L.C. was carried out under the auspices of the Sonderforschungsbereich 608 of the Deutsche Forschungsgemeinschaft. M.S.L. acknowledges financial support from the EPSRC (UK).

[1] N. F. Mott, *Metal-Insulator Transitions* (Taylor & Francis, London, 1974).
[2] M. C. Gutzwiller, Phys. Rev. Lett. **10**, 159 (1963).
[3] J. Kanamori, Prog. Theor. Phys. **30**, 275 (1963).
[4] J. Hubbard, Proc. R. Soc. London, Ser. A **276**, 238 (1963); **281**, 401 (1964).
[5] P. W. Anderson, in *The Theory of Superconductivity in the High-T_c cuprates* (Princeton University Press, Princeton, NJ, 1997).
[6] Q. Si, S. Rabello, K. Ingersent, and J. L. Smith, Nature (London) **413**, 804 (2001).
[7] D. B. McWhan, A. Menth, J. P. Remeika, W. F. Brinkman, and T. M. Rice, Phys. Rev. B **7**, 1920 (1973).
[8] W. Bao, C. Broholm, G. Aeppli, S. A. Carter, P. Dai, T. F. Rosenbaum, J. M. Honig, P. Metcalf, and S. F. Trevino, Phys. Rev. B **58**, 12727 (1998).
[9] C. Castellani, C. R. Natoli, and J. Ranninger, Phys. Rev. B **18**, 4945 (1978).
[10] P. D. Dernier, J. Phys. Chem. Solids **31**, 2569 (1970).
[11] J.-H. Park, L. H. Tjeng, A. Tanaka, J. W. Allen, C. T. Chen, P. Metcalf, J. M. Honig, F. M. F. de Groot, and G. A. Sawatzky, Phys. Rev. B **61**, 11506 (2000).
[12] G. A. Thomas, D. H. Rapkine, S. A. Carter, A. J. Millis, T. F. Rosenbaum, P. Metcalf, and J. M. Honig, Phys. Rev. Lett. **73**, 1529 (1994).
[13] M. J. Rozenberg, G. Kotliar, H. Kajueter, G. A. Thomas, D. H. Rapkine, J. M. Honig, and P. Metcalf, Phys. Rev. Lett. **75**, 105 (1995).
[14] M. Schramme, Ph.D. thesis, Universität Augsburg, 2000.
[15] S.-K. Mo, J. D. Denlinger, H.-D. Kim, J.-H. Park, J. W. Allen, A. Sekiyama, A. Yamasaki, K. Kadono, S. Suga, Y. Saitoh, T. Muro, P. Metcalf, G. Keller, K. Held, V. Eyert, V. I. Anisimov, and D. Vollhardt, Phys. Rev. Lett. **90**, 186403 (2003).
[16] S.-K. Mo, H.-D. Kim, J. W. Allen, G.-H. Gweon, J. D. Denlinger, J.-H. Park, A. Sekiyama, A. Yamasaki, S. Suga, P. Metcalf, and K. Held, Phys. Rev. Lett. **93**, 076404 (2004).
[17] P. Limelette, A. Georges, D. Jérome, P. Wzietek, P. Metcalf, and J. M. Honig, Science **302**, 89 (2003).
[18] J.-H. Park, Ph.D. thesis, University of Michigan, 1994.
[19] T. F. Rosenbaum, A. Husmann, S. A. Carter, and J. M. Honig, Phys. Rev. B **57**, R13997 (1998).
[20] A. Georges, G. Kotliar, W. Krauth, and M. J. Rozenberg, Rev. Mod. Phys. **68**, 13 (1996).
[21] K. Held, I. A. Nekrasov, G. Keller, V. Eyert, N. Blümer, A. K. McMahan, R. T. Scalettar, T. Pruschke, V. I. Anisimov, and D. Vollhardt, in *Quantum Simulations of Complex Many-Body Systems: From Theory to Algorithms*, edited by J. Grotendorst, D. Marks, and A. Muramatsu, NIC Series Vol. 10 (NIC, Jülich, 2002), p. 175.
[22] M. B. Zölfl, Th. Pruschke, J. Keller, A. I. Poteryaev, I. A. Nekrasov, and V. I. Anisimov, Phys. Rev. B **61**, 12810 (2000); K. Held, I. A. Nekrasov, N. Blümer, V. I. Anisimov, and D. Vollhardt, Int. J. Mod. Phys. B **15**, 2611 (2001).
[23] R. Bulla, Adv. Solid State Phys. **40**, 169 (2000).
[24] D. J. García, K. Hallberg, and M. J. Rozenberg, Phys. Rev. Lett. **93**, 246403 (2004).
[25] M. Karski, C. Raas, and G. S. Uhrig, Phys. Rev. B **72**, 113110 (2005).
[26] M. J. Rozenberg, G. Kotliar, and X. Y. Zhang, Phys. Rev. B **49**, 10181 (1994).
[27] M. S. Laad, L. Craco, and E. Müller-Hartmann, Phys. Rev. Lett. **91**, 156402 (2003).
[28] M. S. Laad, L. Craco, and E. Müller-Hartmann, Europhys. Lett. **69**, 984 (2005).
[29] I. V. Solovyev and M. Imada, Phys. Rev. B **71**, 045103 (2005).
[30] K. Held, G. Keller, V. Eyert, D. Vollhardt, and V. I. Anisimov, Phys. Rev. Lett. **86**, 5345 (2001).
[31] S. Yu. Ezhov, V. I. Anisimov, D. I. Khomskii, and G. A. Sawatzky, Phys. Rev. Lett. **83**, 4136 (1999).
[32] M. J. Rozenberg, Phys. Rev. B **55**, R4855 (1997).
[33] V. I. Anisimov, A. I. Poteryaev, M. A. Korotin, A. O. Anokhin, and G. Kotliar, J. Phys.: Condens. Matter **9**, 7359 (1997).
[34] P. Pou, R. Pérez, F. Flores, A. Levy Yeyati, A. Martin-Rodero, J. M. Blanco, F. J. García-Vidal, and J. Ortega, Phys. Rev. B **62**, 4309 (2000); A. Levy Yeyati, F. Flores, and A. Martín-Rodero, Phys. Rev. Lett. **83**, 600 (1999).
[35] H. Kajueter and G. Kotliar, Phys. Rev. Lett. **77**, 131 (1996); see also, A. Levy Yeyati, A. Martín-Rodero, and F. Flores, *ibid.* **71**, 2991 (1993).

[36] S. Biermann, A. Poteryaev, A. I. Lichtenstein, and A. Georges, Phys. Rev. Lett. **94**, 026404 (2005); A. Liebsch, H. Ishida, and G. Bihlmayer, Phys. Rev. B **71**, 085109 (2005).
[37] A. Tanaka, J. Phys. Soc. Jpn. **71**, 1091 (2002).
[38] S. Y. Savrasov, G. Kotliar, and E. Abrahams, Nature (London) **410**, 793 (2001).
[39] J. W. Allen, J. Phys. Soc. Jpn. **74**, 34 (2005).
[40] M. S. Laad, L. Craco, and E. Müller-Hartmann, Phys. Rev. B **64**, 195114 (2001); see also, K. Byczuk, M. Ulmke, and D. Vollhardt, Phys. Rev. Lett. **90**, 196403 (2003).
[41] L. Craco, M. S. Laad, S. Leoni, and E. Müller-Hartmann, Phys. Rev. B **70**, 195116 (2004).
[42] P. Majumdar and H. R. Krishnamurthy, Phys. Rev. Lett. **74**, 3303 (1995).
[43] O. Müller, J. P. Urbach, E. Goering, T. Weber, R. Barth, H. Schuler, M. Klemm, S. Horn, and M. L. denBoer, Phys. Rev. B **56**, 15056 (1997).
[44] G. Keller, K. Held, V. Eyert, D. Vollhardt, and V. I. Anisimov, Phys. Rev. B **70**, 205116 (2004).
[45] V. I. Anisimov, D. E. Kondakov, A. V. Kozhevnikov, I. A. Nekrasov, Z. V. Pchelkina, J. W. Allen, S.-K. Mo, H.-D. Kim, P. Metcalf, S. Suga, A. Sekiyama, G. Keller, I. Leonov, X. Ren, and D. Vollhardt, Phys. Rev. B **71**, 125119 (2005).
[46] P. Pfalzer, G. Obermeier, M. Klemm, S. Horn, and M. L. den-Boer, cond-mat/0508221 (unpublished).
[47] A. Koga, N. Kawakami, T. M. Rice, and M. Sigrist, Phys. Rev. Lett. **92**, 216402 (2004).
[48] S. Biermann, L. de' Medici, and A. Georges, Phys. Rev. Lett. **95**, 206401 (2005).
[49] V. I. Anisimov, I. A. Nekrasov, D. E. Kondakov, T. M. Rice, and M. Sigrist, Eur. Phys. J. B **25**, 191 (2002).
[50] J. W. Allen, Phys. Rev. Lett. **36**, 1249 (1976).